C. R. Chimie 18 (2015) 834–847

Contents lists available at ScienceDirect

Comptes Rendus Chimie

www.sciencedirect.com

Full paper/Mémoire

Selective production of propylene from methanol over high-silica mesoporous ZSM-5 zeolites treated with NaOH and NaOH/tetrapropylammonium hydroxide

Javad Ahmadpour, Majid Taghizadeh *

Chemical Engineering Department, Babol University of Technology, P.O. box 484, 4714871167 Babol, Iran

ARTICLE INFO

Article history:
Received 20 February 2015
Accepted after revision 7 May 2015
Available online 15 July 2015

Keywords:
Hierarchical porosity
High-silica ZSM-5
Methanol-to-propylene (MTP)
Desilication
Selectivity

ABSTRACT

The influence of alkaline treatments with NaOH and NaOH/TPAOH mixtures on the physicochemical properties and catalytic performance of high-silica ZSM-5 zeolites (Si/Al = 175) during the methanol-to-propylene (MTP) reaction have been investigated. It was found that alkaline treatment in an NaOH/TPAOH solution with TPAOH/(NaOH + TPAOH) = 0.4 ensures the formation of narrow and uniform intracrystalline mesoporosity without severely damaging the crystal structure and the intrinsic acidity of the zeolite, leading to the best catalytic performance, including the highest propylene selectivity (47.2) and P/E ratio (4.97) as well as the longest catalyst lifetime (80 h).

1. Introduction

In modern petrochemical industry, propylene is one of the most important intermediates for the production of polypropylene, polyacrylonitrile, acrolein, and acrylic acid. Currently, propylene is mostly produced as a byproduct of both the petroleum refinery in fluid catalytic cracking (FCC) units and the ethylene generation by naphtha steam cracking. Due to the increasing global demand for propylene and the shortage of petroleum resource in the future, new processes with high yield of propylene are required [1,2]. Both methanol-to-olefins (MTO) and methanol-to-propylene (MTP) processes are prominent alternative routes for producing propylene from non-petroleum resources, since methanol can be economically produced from natural gas and coal on a large scale [3–5]. The MTO technology has been commercialized by UOP/Hydro for producing both ethylene and propylene based on a SAPO-34 catalyst in a fluidized bed rector, whereas the MTP process has been developed by Lurgi to produce propylene preferentially based on a ZSM-5 catalyst in a fixed-bed reactor [6,7]. Hence, the MTP process might be the most desirable route to fill up the growing gap between the supply and the demand of propylene. The first MTP plant was established in China in 2010 [8].

Over the past decades, extensive studies have been done on the activity and selectivity of methanol conversion over ZSM-5 zeolite with different Si/Al ratios, and concluded that the high-silica ZSM-5 zeolite is a very promising candidate for the catalysis of methanol to propylene due to its high selectivity towards propylene as well as its long catalytic lifetime [2,9–11]. Despite these superior results, the relatively small micropores in ZSM-5 zeolites significantly influence the mass transfer of the reactants and products towards and away from the active sites, which would result in relatively easy coke formation and subsequently limit the performance of the industrial catalysts [12,13]. Hence, the modification of the ZSM-5 zeolite to optimize the activity and selectivity in the MTP reaction still remains a key challenge in state-of-the-art catalysis research.

* Corresponding author.
E-mail address: m_taghizadehfr@yahoo.com (M. Taghizadeh).

http://dx.doi.org/10.1016/j.crci.2015.05.002
1631-0748/

One strategy to solve the problem of rapid deactivation and develop a highly stable catalyst for the MTP reaction consists in introducing substantial intra- and/or intercrystalline mesoporosity (i.e., pores with diameters ranging between 2 and 50 nm) besides the intrinsic micropore system, which are usually referred to as mesoporous ZSM-5 or hierarchical ZSM-5 [2,12,14]. The added mesoporosity decreases the intracrystalline diffusion limitations and increases the accessibility to active sites, resulting in an improved catalytic performance. A wide variety of methods are presently available to prepare hierarchical porous ZSM-5, including templating techniques (bottom-up) and post-synthesis modification of microporous ZSM-5 (top-down) [15,16].

Among the post-synthesis treatments, desilication of ZSM-5 in alkaline solutions (typically NaOH) has been proved to be the most promising one, in terms of simplicity, versatility, and efficiency. Nevertheless, the application of desilication by an aqueous NaOH solution is limited to zeolites with a Si/Al ratio in the range of 25–50 [17–28]. Recently, the desilication of high-silica ZSM-5 and silicalite-1 has attracted much attention. However, the major drawback of this treatment is uncontrolled silicon extraction, resulting in the loss of a significant part of the zeolite structure [19]. To overcome this problem, the addition of a pore-directing agent (PDA) such as tetraalkylammonium cations along with NaOH has been proposed as an effective alkaline treatment for introducing intracrystalline mesopores in zeolites with a high Si/Al ratio or even in the case of pure silica zeolitic materials. The alkaline treatment of silicalite-1 in the presence of the tetrapropylammonium cation (TPA^+) led to a higher surface area as well as a higher pore volume due to a smaller mesopore size, whereas the crystallinity and microporosity were better preserved than in the case when pure NaOH was used [19,29]. Moreover, in the case of high-silica ZSM-5, using the mixture of NaOH and TBAOH (tetrabutylammonium hydroxide) as a leaching agent led to the formation of narrower and more uniform mesopores as well as to a significant increase in the accessibility of the active sites, compared to using NaOH alone [30].

Catalytic performance of inorganic alkaline-treated ZSM-5 during the conversion of methanol to hydrocarbon (MTH) has been recently investigated in a number of open literatures in which the main attribute of mesoporous zeolites is a prolonged catalyst lifetime in comparison to their conventional counterparts [31,32]. Bjørgen et al. [33] reported a significant improvement in the catalyst lifetime of ZSM-5 as well as a strongly increased selectivity towards the desired gasoline fraction in the methanol-to-gasoline (MTG) reaction after alkali treatment of ZSM-5 with NaOH. The results were rationalized by alterations of acidic properties, mesopore formation, and improved diffusivity. Mei et al. reported that the mesopore formation through alkaline desilication treatment of ZSM-5 zeolite with Si/Al ratio of 72 led to enhanced propylene selectivity up to 42% as well as an increase in the ratio of propylene to ethylene to 10:1 in the catalytic conversion of methanol to propylene [2].

At present, organic alkaline-treated ZSM-5 is also used as a catalyst in methanol conversion reactions. The organic alkaline treatments incorporate more moderate modifications and are more easily controlled compared with inorganic ones. He et al. investigated the effect of the TPAOH treatment duration on the catalytic performance of nanocrystalline ZSM-5 in the MTG reaction, and concluded that the stability of the modified catalyst increased by extending the TPAOH treatment time [34]. Moreover, Li et al. [35] modified a low-silica ZSM-5 zeolite in a mixed alkaline aqueous solution of TPAOH and NaOH, and found that this treatment with proper TPA^+/OH^-ratio could increase the propylene selectivity of the modified zeolite in the MTO reaction.

However, to the best of our knowledge, the catalytic performance of a high-silica mesoporous ZSM-5 prepared by mixed alkaline treatment (TPAOH/NaOH) in the MTP reaction has not been previously reported. Hence, the aim of this work was to investigate the influence of alkaline treatments with different combinations of NaOH and TPAOH solutions on the mesoporosity of a highly siliceous ZSM-5 zeolite (Si/Al = 175) and their catalytic performance in MTP reaction. To get a better understanding of the relation between the mesoporosity and the catalytic performance of mesoporous ZSM-5, a conventional microporous ZSM-5 was employed for comparison. The physicochemical properties of the parent and treated zeolites were characterized by XRD, ICP-OES, FE-SEM, BET, and NH_3-TPD methods. Meanwhile, their catalytic performance was also evaluated for the MTP reaction using a fixed-bed flow reactor under the same operating conditions. A number of findings is presented, which have not been reported earlier.

2. Experimental

2.1. Materials

Tetrapropylammonium hydroxide (TPAOH, 40 wt.% aqueous solution), tetraethyl orthosilicate (TEOS, 98 wt.%), sodium hydroxide (99 wt.%), ammonium nitrate (99 wt.%), and methanol (99.5 wt.%) were purchased from Merck, while aluminum isopropoxide (AIP, 97 wt.%) was purchased from Aldrich. All chemical reagents were of analytical grade and used as received without further purification.

2.2. Catalyst preparation

2.2.1. Parent zeolite synthesis

A parent ZSM-5 zeolite with SiO_2/Al_2O_3 molar ratios of 350 was prepared using the hydrothermal procedure [36]. In a typical synthesis procedure, firstly, the calculated amounts of aluminum isopropoxide (AIP) and TPAOH were mixed with double-distilled water in a polypropylene bottle under magnetic stirring for about 15 min until AIP was completely dissolved in the solution. Next, TEOS was added dropwise to the resultant mixture in order to achieve a molar composition of SiO_2: (1/350) Al_2O_3: 0.3 TPAOH: 15 H_2O. The obtained mixture was continuously stirred at room temperature for 3 h to ensure complete hydrolysis of TEOS and AIP to ethanol and isopropyl alcohol, respectively. Then, the final mixture was transferred into a homemade Teflon-lined stainless-steel

autoclave (100 mL, *ca.* 80% filled) for hydrothermal treatment at 180 °C for 72 h under autogenous pressure. Afterwards, the zeolite suspension was immediately quenched to room temperature by immersion of the autoclave in an ice water bath to terminate crystallization. Subsequently, the solid product was collected by filtration, washed several times with double-distilled water until a neutral pH value was obtained, dried in an oven at 110 °C overnight, and finally calcined in a quartz tube furnace under flowing air at 550 °C for 6 h to remove the organic template completely. The final sample is designated as the parent.

2.2.2. Alkaline treatment

Alkaline treatments of parent ZSM-5 sample were performed by either a pure NaOH solution or a mixture of NaOH and TPAOH (tetrapropylammonium hydroxide) in a round-bottom flask coupled with a reflux condenser. The concentration of either solution was 0.2 M. The alkaline-treated samples were designated as ATZ-*x*R, in which *x* refers to the molar TPAOH/(NaOH + TPAOH) ratios (denoted as *R*). For a pure NaOH solution, *x* was 0.0 and for the TPAOH/NaOH mixtures, *x* was varied from 0.2 to 0.6. For each test, 90 mL of the alkaline solution were stirred magnetically at 400 rpm and heated to 65 °C by means of an oil bath. Afterwards, 3 g of zeolite were added. The resulting mixture was left to react under reflux for 30 min. After desilicating, the zeolite suspension was cooled down immediately using an ice water bath, and filtered. At this stage, a portion of collected filtrate was taken for analysis. The filtration cake was washed with deionized water until a neutral pH value was obtained and finally dried at 100 °C overnight. The dried sample was transformed into ammonium form by three-fold ion exchange with 1 M NH_4NO_3 at 80 °C for 2 h. Afterwards, the sample was again filtrated, washed, and dried overnight, Eventually, the dried sample was converted into the hydrogen form through calcination, following the program described for the parent sample.

2.3. Characterization

X-ray diffraction (XRD) patterns of different samples were obtained with a PANalytical X'Pert PRO MPD, using a Cu Kα_1 radiation source (λ = 1.5406 A°) at room temperature with instrumental settings of 40 kV and 40 mA. Data were recorded in the 2θ range from 5° to 50° with a step size of 0.026°.

The content of silicon and aluminum in the filtrates was determined by inductively coupled plasma-optical emission spectroscopy (ICP-OES). The measurements were performed using a Perkin Elmer Optima 2000 DV ICP-OES.

N_2 adsorption-desorption isotherms at 77 K were measured using a NOVA 2200 instrument (Quantachrome, USA) in the relative pressure range from 0.05 to 0.99. Prior to N_2-physisorption measurements, the samples were degassed at 473 K in an N_2 flow for 16 h in order to remove the moisture adsorbed at both the surface and the internal pores. Total specific surface areas (S_{BET}) were calculated using the Brunauer-Emmett-Teller (BET) method in the p/p_0 range 0.05–0.25, and the total pore volume was estimated from the amount of nitrogen adsorbed at a relative N_2 pressure (p/p_0) of 0.99. The *t*-plot method was employed to evaluate the micropore surface area (S_{Micro}) and the micropore volume (V_{Micro}) in the p/p_0 range 0.1–0.4. The mesopore volume (V_{Meso}) was calculated from the discrimination between the V_{Tot} and V_{Micro}. The mesopore size distributions and the average diameter of mesopores were estimated by using the Barrett-Joyner-Halenda (BJH) method from the desorption branch of the isotherms.

The morphology and particle size measurements were carried out using a field-emission scanning electron microscope (FE-SEM Model: MIRA3 TESCAN, USA) operating at 15 kV. All samples were subsequently sputter coated with a thin gold film to reduce the charging effects.

The acidity of the samples was measured by temperature-programmed desorption of ammonia (NH_3-TPD) using BELCAT-A instrument (Bel Japan, Inc.) with a conventional flow apparatus which included an online thermal conductivity detector (TCD). In a typical analysis, 35 mg of the sample were initially flushed with helium at 300 °C for 2 h at a heating rate of 10 °C/min and then cooled down to 60 °C and further saturated with NH_3. After NH_3 exposure, the sample was purged with helium for 30 min to remove weakly and physically adsorbed NH_3 on the surface of the catalyst. After these operations, the sample was heated from 35 to 850 °C at a heating rate of 5 °C/min and the amount of ammonia in the effluent was measured via TCD and recorded as a function of temperature.

2.4. Catalytic performance

The performance of the catalysts for the methanol-to-propylene reaction was investigated in a fixed-bed reactor under atmospheric pressure at 460 °C. A schematic view of the lab scale setup is shown in Fig. 1. The reactor was made of a stainless-steel tube with an inner diameter of 8 mm and a length of 70 cm, which was electrically heated by a vertical three-zone tube furnace (PTF 12/75/750, Lenton Ltd, UK). Before testing the catalytic activity, the catalyst powder was pelletized at 10 ton for 10 min, crushed and sieved to obtain 18–25 mesh particles. For each test, 1 g of mesh catalyst was loaded into the middle of the isothermal zone of the reactor. In addition, to prevent back-mixing and homogenization of gas flow on the catalyst bed, inert quartz particles (12–16 mesh) were filled upstream and downstream of the catalyst packing of the reactor.

A K-type thermocouple was positioned coaxially in the center of the catalyst bed in order to monitor the reaction temperature. Prior to the start of the MTP reaction, the sample was activated in situ at a heating rate of 3.5 °C/min under highly purified N_2 flow (30 mL·min^{-1}) and under atmospheric pressure. When the catalytic bed temperature reached 550 °C, it was maintained at that temperature for 2 h. After cooling to the reaction temperature in flowing nitrogen, a mixture of 50 wt.% methanol in water with methanol WHSV = 1 h^{-1} was pumped through a HPLC pump (Knauer Smartline 1000; Germany) to an in-house-built preheater operating at 150 °C before being fed to the reactor. The reactor outlet stream was cooled to 10 °C in a refrigeration bath and then the gas and the liquid products were separated. To avoid possible condensation of heavy compounds, the transfer line from the reactor outlet to the

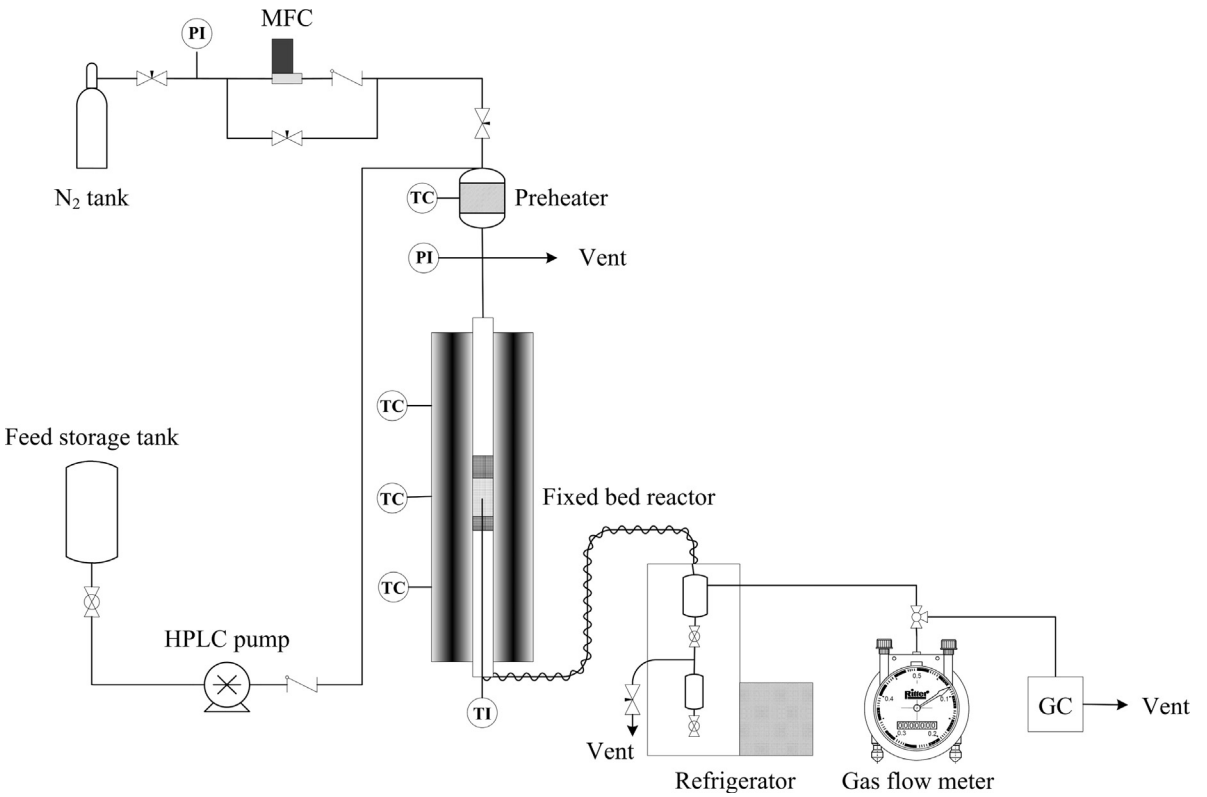

Fig. 1. A schematic view of the lab scale setup.

refrigeration bath was externally heated and maintained at 170 °C. The gas phase was sent to a gas flow meter (Ritter TG 05, Germany) and an online gas chromatograph (Varian 3800), equipped with a flame ionization detector (FID) and a 50-m HP-PONA capillary column. The liquid products were collected after each 6-h reaction period, weighted, and analyzed off-line in the same gas chromatograph used for online analyses.

Then the reaction performance results, including methanol conversion and hydrocarbon products selectivities, were calculated. Due to very fast equilibrium reaction of methanol to DME, those two species can be combined as one lumped reactant species (oxygenates) in the calculation of conversion and hydrocarbon products' selectivities. Hence, the conversion of methanol in the MTP reaction was calculated through the following equation:

$$\textit{Methanol conversion} = \frac{N^{i}_{MeOH} - (N^{o}_{MeOH} + 2N^{o}_{DME})}{N^{i}_{MeOH}} \times 100 \quad (1)$$

The product selectivity was defined as the mole ratio of each product (on a CH_2 basis referred to the moles of converted methanol):

$$\text{Selectivity} = \frac{xN^{o}_{C_xH_y}}{N^{i}_{MeOH} - (N^{o}_{MeOH} + 2N^{o}_{DME})} \times 100 \quad (2)$$

where superscript *i* refers to the components at the inlet of reactor and superscript *o* refers to the components at the reactor outlet; subscript *x* refers to the number of carbon atoms.

3. Results and discussion

3.1. Physicochemical properties of the parent and alkaline-treated ZSM-5 catalysts

XRD analysis was performed to investigate the possible structural changes in the ZSM-5 zeolite. XRD patterns of the parent and all desilicated ZSM-5 zeolites are shown in Fig. 2, from which it can be seen that the intrinsic MFI structure was preserved and that no additional phase was formed during alkaline treatment under the experimental conditions.

The XRD technique is also used to assess the change in relative crystallinity of the alkaline-treated samples. The relative crystallinity was calculated according to procedure A described in ASTM D5758-01 [37]. This calculation is based on the ratio of the integrated peak areas between $2\theta = 22.5°$ and 25° of the desilicated sample relative to those of the parent ZSM-5 sample as the reference sample (whose crystallinity is regarded as 100%). Table 1 reports the relative crystallinity of the desilicated samples.

The results confirmed that desilication of ZSM-5 with NaOH or an NaOH/TPAOH mixture practically did not disturb the long-range crystallinity of the resulting materials, although the alkaline treatment of the zeolite is accompanied by a preferential removal of siliceous species (Table 1). A likely explanation for these observations is that

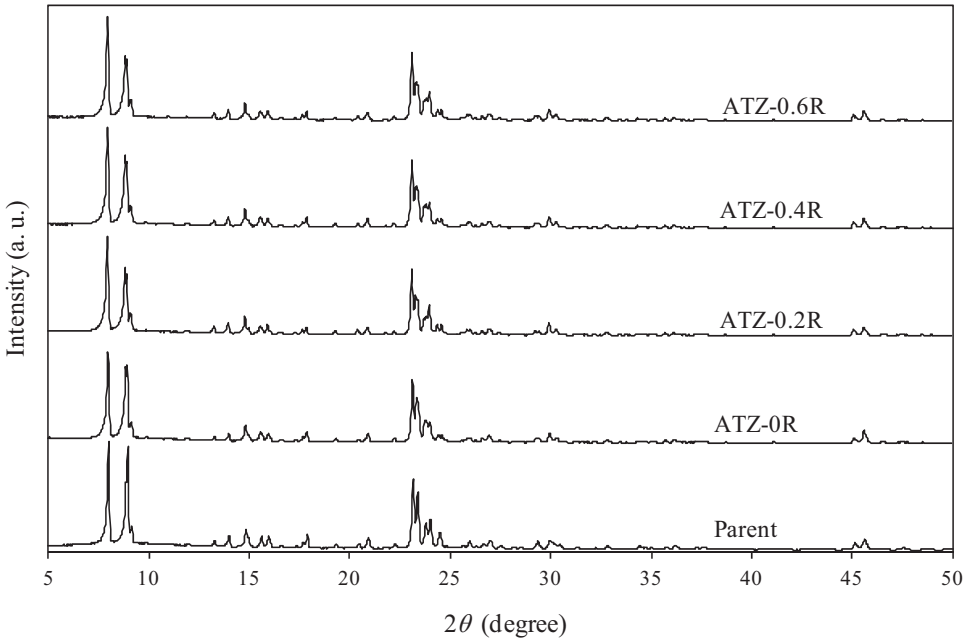

Fig. 2. XRD patterns of the parent and desilicated ZSM-5 samples.

the amorphous phase or less crystalline material in the parent sample is specifically removed by alkali solutions without significant destruction of the zeolite framework. Hence, with respect to XRD, the parent and desilicated samples are nearly similar. This is in line with expectations, since previous studies have reported similar observations on mesoporous structures [30,33].

It is worth noticing that the alkaline treatment of ZSM-5 leads to the dissolution of both framework silicon and framework aluminum. However, since the Si–O–Si bond is easier to hydrolyze than the Si–O–Al bond in the zeolite framework, the dissolution of framework Si is favored over that of framework Al in the alkaline medium. This is generally due to the fact that the negative charge of AlO_4^- tetrahedra in the zeolite framework hinders the extraction of Al through hydrolysis of Si–O–Al bonds by negatively charged hydroxyl ions. Moreover, it is generally accepted that the presence of AlO_4– protects the neighboring Si atoms against OH attack. As a result, in high-silica ZSM-5 (Si/Al = 175), due to low concentration of neighboring Al tetrahedra, the attack of the hydroxyl ions to the surface Si atoms is not hindered by any negative charge. Therefore, a preferential removal of siliceous species occurred during the alkaline treatments. The analysis of filtrates confirmed the high selectivity of alkaline treatments for silicon extraction in our experimental conditions, and, as expected, a higher amount of Si was leached during the treatment with pure NaOH (1133 ppm) in comparison to the treatment in an NaOH/TPAOH mixture. Less extensive desilication of high-silica zeolites in the presence of TPAOH is assigned to its protective influence on zeolite structure, resulting from the known affinity of TPA^+ cations to the zeolite surface. Nevertheless, the amounts of aluminum leached from the high-silica zeolite treated with an NaOH/TPAOH mixture are higher than that of samples treated with pure NaOH (Table 1). This is ascribed to the adsorption of TPA^+ onto the zeolite, sealing off most of the available external surface, hereby largely inhibiting surface realumination, contrary to what occurs in pure NaOH [38–40].

Table 1
Chemical composition of filtrates and crystallinity of the parent and alkaline-treated ZSM-5 catalysts.

Sample name	$Si_{filtrate}$[a] (ppm)	$Al_{filtrate}$[a] (ppm)	Crystallinity[b]
Parent	–	–	100
ATZ-0R	1133	1.6	90
ATZ-0.2R	473	16	93
ATZ-0.4R	320	16	95
ATZ-0.6R	264	17	97

[a] Determined by inductively coupled plasma-optical emission spectroscopy (ICP-OES).

[b] Relative crystallinity calculated based on the sum of peak areas between $2\theta = 22.5^\circ$ and 25° from XRD pattern of alkaline-treated ZSM-5 samples compared to that of parent ZSM-5100% crystalline (ASTM D5758-01).

Hence, upon alkali treatment, mainly silicon species are removed from the surface or bulk of the ZSM-5 zeolites. This removal causes the formation of mesopores in the nanometer range (Fig. 3) coupled with a substantial mesopore volume. The removal of silicon species from the zeolites also leads to changes in their surface area, pore size distribution, and pore volume [17–19,29,30]. N_2 adsorption-desorption isotherms and the corresponding BJH pore size distribution (PSD) curves of the parent and the alkali-treated ZSM-5 zeolites are illustrated in Figs. 3 and 4, respectively, and their textural properties are summarized in Table 2. Looking at the nitrogen isotherms, the parent ZSM-5 exhibits only a representative type-I isotherm, which is characteristic of microporous materials without significant mesoporosity. This is verified by its BJH

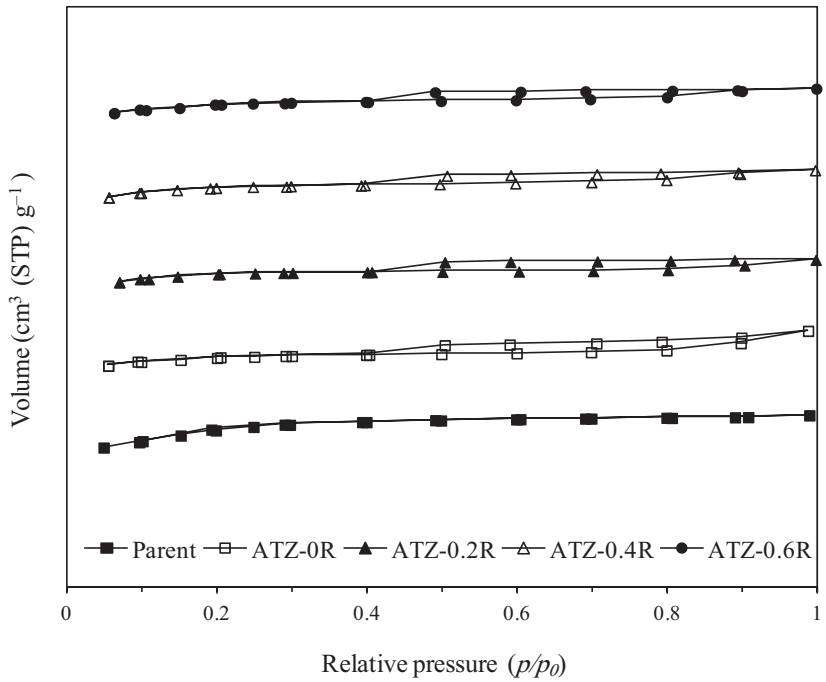

Fig. 3. N_2 adsorption-desorption isotherms of the parent and alkaline-treated ZSM-5 samples.

pore size distribution curve (Fig. 4), where there is no obvious peak in the mesoporous range. As listed in Table 2, the BET surface area and total pore volume of parent ZSM-5 are 345 $m^2 g^{-1}$ and 0.178 $cm^3 g^{-1}$, while the mesoporous surface area and pore volume are very low, only 35 $m^2 \cdot g^{-1}$ and 0.042 $cm^3 \cdot g^{-1}$, respectively. On the other hand, ATZ-*x*R series samples exhibited a type-IV isotherm with an obvious hysteresis loop at a relative pressure higher than $p/p_0 = 0.4$, indicating the formation of a hierarchical porous system combining micro- and mesoporosity. These hysteresis loops are usually associated with the capillary condensation of nitrogen within the mesopores. Moreover,

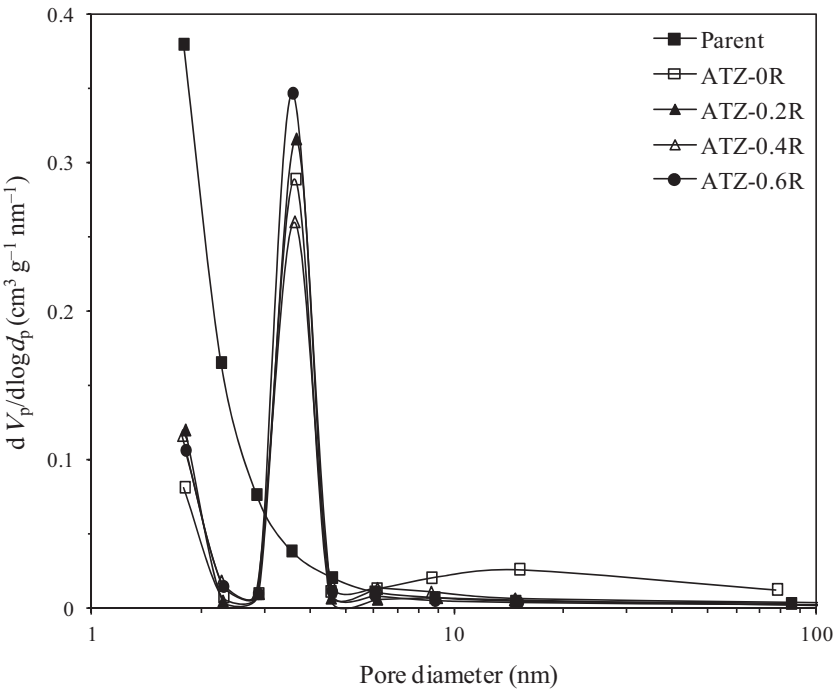

Fig. 4. BJH pore size distribution curves of the parent and alkaline-treated ZSM-5 samples.

Table 2
Textural properties of the parent and alkaline-treated ZSM-5 samples.

Sample name	Surface area ($m^2 \cdot g^{-1}$)			Pore volume ($cm^3 \cdot g^{-1}$)			HF[g]
	S_{BET}[a]	S_{Micro}[b]	S_{Meso}[c]	V_{Total}[d]	V_{Micro}[e]	V_{Meso}[f]	
Parent	345	310	35	0.178	0.136	0.042	0.077
ATZ-0R	397	256	141	0.221	0.113	0.108	0.182
ATZ-0.2R	394	265	129	0.201	0.116	0.085	0.190
ATZ-0.4R	404	253	151	0.209	0.109	0.100	0.195
ATZ-0.6R	400	259	141	0.205	0.112	0.093	0.193

[a] BET surface area.
[b] Micropore surface area evaluated by *t*-plot method.
[c] Mesopore surface area calculated using S_{BET}–S_{Micro}.
[d] Total pore volume at $p/p_0 = 0.99$.
[e] Micropore volume calculated by the *t*-plot method.
[f] Mesopore volume calculated using V_{Total}–V_{Micro}.
[g] The hierarchy factor.

the largely parallel displacement of the adsorption and desorption branches of the hysteresis loop indicates the presence of open (cylindrical) mesopores connected to the outer surface [39]. However, the changes in the hysteresis loops of the samples treated with the NaOH/TPAOH mixture are less obvious than in the case when pure NaOH is used, which may be due to a gentler modification by the NaOH/TPAOH mixture than by pure NaOH. This supports the difference between the mesopore size distributions of the materials desilicated with different alkaline solutions (pure NaOH or NaOH/TPAOH mixtures), as shown in Fig. 4. The samples treated with a mixture of NaOH/TPAOH exhibits a narrow and uniform mesopore size distribution centered at ~3.6 nm. There is no significant difference in mesopore size distributions for the materials treated with NaOH/TPAOH mixtures at various proportions between both bases. This is in line with the results obtained by Sadowska et al., who focused on the desilication of high-silica ZSM-5 with NaOH/(TBAOH) mixtures [30]. In contrast, the sample treated with pure NaOH reveals a bimodal mesopore size distribution, with a narrow peak centered at ~3.6 nm and a tiny broad peak centered at ~15 nm. Sadowska et al., who focused on the desilication of high-silica ZSM-5 with NaOH, also observed a similar peak at ~15 nm [30].

The formation of mesopores within the zeolite structure is also confirmed by FE-SEM images of parent and desilicated samples. As clearly shown in Fig. 5a, the crystals size of the parent ZSM-5 is large, and their surfaces are quite smooth, which confirms the absence of mesopores in its structure. But the alkaline treatment causes a significant change in the surface of the parent zeolite. Additionally, distinct differences can be seen between the morphologies of the ZSM-5 zeolites desilicated with pure NaOH and with NaOH/TPAOH mixtures, indicating that the desilication mechanism of NaOH/TPAOH is different from that in NaOH media. As seen in Fig. 4c, the sample treated with an NaOH/TPAOH mixture ($R = 0.4$) shows more uniform intracrystalline mesopores that spread through the entire surface of the ZSM-5 crystal, whereas the crystal shape remains preserved, indicating that the silicon species has been removed properly. The existence of these surface open holes is probably the main cause for the facilitation of molecular transport in MTP reaction and the improvement of the catalytic performance of the ZSM-5 catalysts [2]. So, its effect on the catalyst performance in the MTP reaction is worthy to be further investigated.

However, during the alkaline treatment with pure NaOH, not only the large crystals of parent ZSM-5 are broken down into smaller ones, but also some grooves and voids appear on the surface of ZSM-5 fragments (Fig. 5b). As a result, this treatment leads to the formation of hierarchical ZSM-5 with both intra- and intercrystalline mesoporosity, which is in accordance with its BJH pore size distribution curve obtained from N_2 adsorption-desorption isotherms.

The textural properties derived from N_2 isotherms (Table 2) also reveal that the mesoporosity (both mesopore surface area and volume) of the alkali-treated samples increases without significant change in their micropores volume, even for the treatment with pure NaOH alkaline solutions, which causes the massive dissolution of the zeolite crystals. This means that although alkaline leaching with pure NaOH leads to the fragmentation of the zeolite crystals, each fragment preserves its microporosity. It is in line with those reported by other researchers who also focused on the desilication of high-silica ZSM-5 with NaOH and NaOH/(TBAOH) mixtures [30], and is in agreement with the evolution of the crystallinity assessed by XRD previously discussed.

It is also interesting to note that the sample treated with pure NaOH exhibits the highest value of mesopore volume ($0.108\ cm^3 \cdot g^{-1}$), whereas the largest mesopore surface area ($151\ m^2 \cdot g^{-1}$) is obtained upon the alkaline treatment with an NaOH/TPAOH mixture ($R = 0.4$). In other words, although the largest mesopore volume is achieved for ATZ-0R, possibly due to the existence of both intra- and intercrystalline porosity in this sample (Figs. 4 and 5b), its surface area is smaller than that of ATZ-0.4R. This indicates that the mesoporosity was not properly developed in the high-silica ZSM-5 (Si/AL = 175) during alkaline treatment with pure NaOH, which is again confirmed by FE-SEM micrograph (Fig. 5b). The low effectiveness of pure NaOH treatment for mesoporosity introduction in a high-silica ZSM-5 was also reported by others [17,19,30].

On the contrary, the desilication of high-silica ZSM-5 by NaOH/TPAOH mixture not only results in the formation of narrower and uniform mesopore size distribution but also

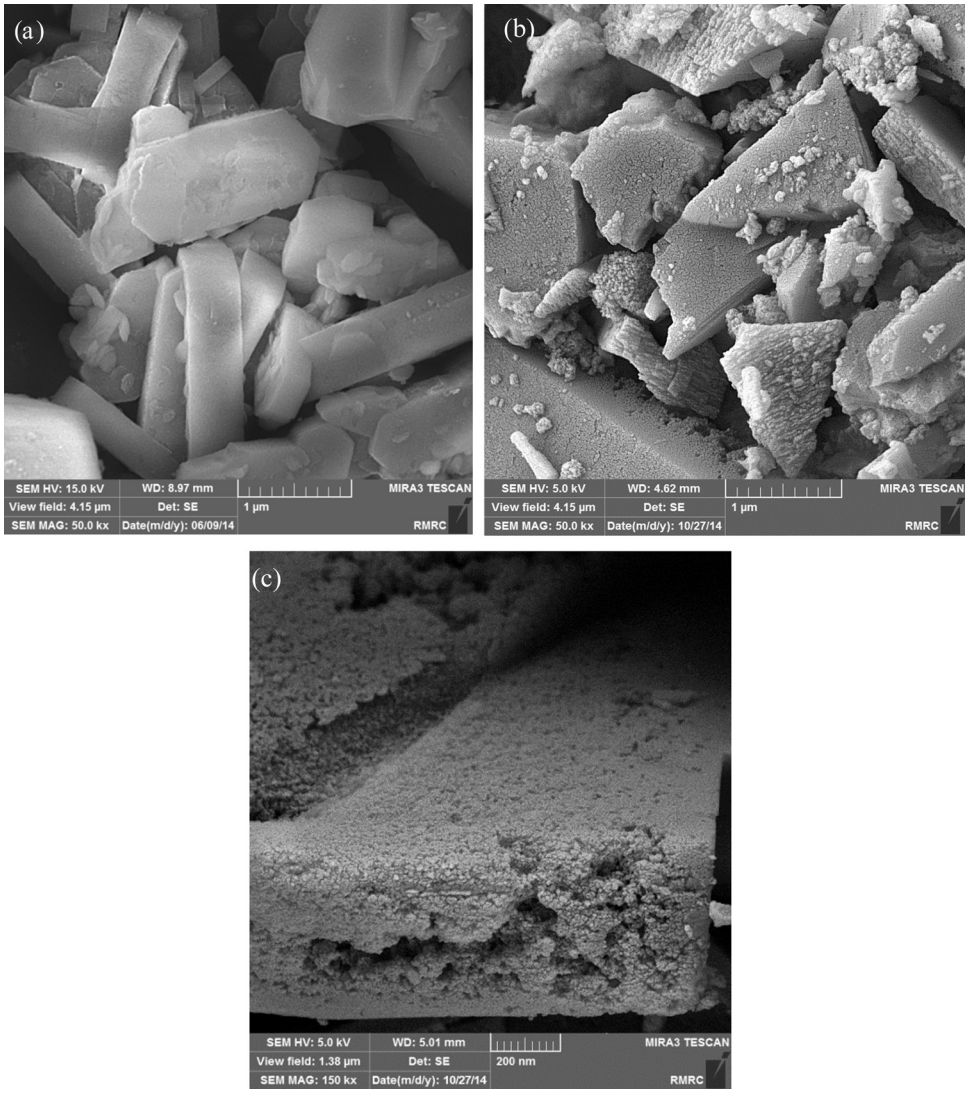

Fig. 5. FE-SEM images of the parent and selected alkaline-treated ZSM-5 samples.

leads to substantial modifications of both pore volume and specific surface area in comparison with parent zeolites. However, the textural parameters of the treated zeolites with NaOH/TPAOH mixtures depend on the TPAOH/(TPAOH + NAOH) molar ratio (denoted by R). According to the data listed in Table 2, whether desilication was done at low or high TPAOH level in the desilicating mixture ($R = 0.2$ or 0.6), the increase in both pore volume and surface area was less significant than in the case when pure NaOH was used. The largest BET and mesoporous surface area were obtained for the sample treated with TPAOH/(NaOH + TPAOH) = 0.4, although its mesopore volume is slightly smaller than that of the sample treated with NaOH only ($R = 0$).

The attractiveness of a hierarchical zeolite is often related to its mesopore volume (V_{meso}) or mesopore surface area (S_{meso}). A quantified comparison of the zeolites in terms of all four textural parameters is made by making use of the hierarchy factor (hereafter referred to as HF). This factor, defined as $(V_{Micro}/V_{Total}) \times (S_{Meso}/S_{BET})$, is one of the most powerful tools to describe the porosity of the hierarchical zeolites [29], so that its maximized value is highly desired. The final column of Table 2 summarizes the obtained HFs. Going from sample parent to ATZ-0.4R, HF increases from 0.077 to its maximum value, i.e. 0.195, which indicates that the increase in the relative mesoporosity (S_{meso}/S_{BET}) is larger than the decrease in relative microporosity (V_{micro}/V_{total}). On the other hand, the mesopore formation process is negatively influenced by a very high amount of TPAOH in the system ($R = 0.6$), taking into account the reduced HF value of ATZ-06R (0.193). Hence, 40% of TPAOH in the desilicating mixture ($R = 0.4$) is the proper amount of PDA allowing us to reach the maximum mesoporosity with minimum loss of microporosity.

The difference between the mesoporosity and the textural properties of the materials desilicated with different alkaline solutions can be explained by considering

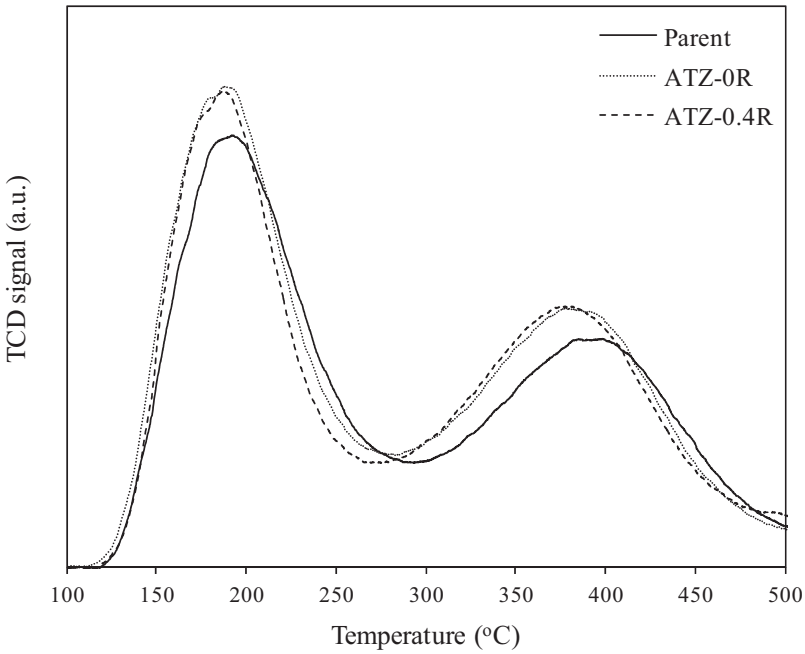

Fig. 6. NH_3-TPD profiles of the parent and selected alkaline-treated ZSM-5 samples.

the role of pore-directing agents (PDAs). According to the literature [19], both Al extracted from ZSM-5 framework in the desilication process and tetrapropylammonium cation (TPA^+) act as a pore-directing agent (PDA), largely protecting the zeolite crystals against OH ions attack and the massive dissolution during the desilication process. Several results [19,30,40] reported that larger pores were observed in the presence of Al in the desilication mixture, whereas smaller pores were formed with amine hydroxides as PDA. As a high-silica ZSM-5 (Si/Al = 175) was used in our study, the amount of Al extracted into the alkaline solution was negligible, so that only TPA^+ played the role of PDA. The presence of TPA^+ cations in the alkaline medium promotes the formation of narrow and uniform secondary mesopores within the ZSM-5 crystals in comparison to the treatment in pure NaOH solution. Consequently, the samples desilicated with NaOH/TPAOH mixture have well-spread hierarchical systems, as found in Fig. 5c and Table 2. Such protective influence of TPAOH on the zeolite structure can be explained by the fact that the TPA^+ binds to the surface of the zeolite in alkaline medium. It is therefore expected that with increasing TPA^+ concentration in the system, a monolayer is formed on the external surface of the zeolite, which fulfills the pore-directing role by controlling the dissolution of zeolite crystals. These results are consistent with the earlier findings concerning the mechanism of desilication in the presence of PDAs. On the other hand, in the absence of the PDA, the reaction of the OH^-anions with the zeolitic framework predominates at the external surface of the zeolite, leading to uncontrolled silicon dissolution and consequently to the formation of larger and irregular pores [19,29,30,40].

Acidity changes in the samples upon alkaline treatments were investigated by the NH_3-TPD method. The acidity is viewed as a vital factor in determining the catalytic performance in the MTP reaction. Fig. 6 presents the NH_3-TPD profiles of the parent and selected alkali-treated ZSM-5 zeolites (ATZ-0R and ATZ-0.4R). The acidities of selected catalysts determined from TPD peak areas and the strength of acid sites corresponding to desorption peaks temperatures are summarized in Table 3. As shown in Fig. 6, two distinct NH_3 desorption peaks are observed in the NH_3-TPD profiles of the catalysts: a low-temperature peak (T_{d1}) at around 185–190 °C and a high-temperature peak (T_{d2}) at around 375–395 °C corresponding to the weak and the strong acid sites, respectively. These results are in line with the reported literature data for the acidity of MFI materials [41,42]. Although NH_3-TPD analysis cannot discriminate between Brønsted and Lewis acidity, the low-temperature peak is attributed to ammonia desorption from weak Lewis acid sites, whereas the high-temperature peak is related to ammonia desorbed from stronger Brønsted acid sites [43]. It is extensively believed that weak acid sites have little activity in methanol conversion to light olefins, whereas strong acid

Table 3
The NH_3-TPD data for the parent and selected alkaline-treated ZSM-5 samples.

Catalyst	Distribution and concentration of acid sites (mmol NH_3/g)			Peak temperature (°C)	
	Region I	Region II	Total	T_{d1}	T_{d2}
	Weak	Strong			
Parent	0.071	0.064	0.135	189	392
ATZ-0R	0.085	0.072	0.157	188	383
ATZ-0.4R	0.075	0.076	0.151	187	376

sites on the ZSM-5 catalyst surface are known as MTH catalytic centers [44,45].

Compared with the parent sample, the number of both weak and strong acid sites in the alkali-treated samples (ATZ-0R and ATZ-0.4R) is relatively increased. Such enhancement in the acid sites is accordingly attributed to the increased Al concentration after the preferential desilication, which gives a higher density of acid sites. Other groups also reported the increase of the relative aluminum content in the alkali-treated zeolites [24,46]. Moreover, the predominating intracrystalline mesoporosity of the zeolites desilicated with NaOH/TPAOH mixture (Figs. 4 and 5c) may lead to the coverage of Brønsted acid sites in the pore mouth regions, resulting in their high accessibility [26]. It was also reported by Sadowska et al. that the full accessibility of the protonic sites after treatment with NaOH/TBAOH mixture could be the result of the creation of predominating intraparticle mesoporosity [27,30].

Additionally, it can be seen from Table 3 that the amounts of the weak acid sites on ATZ-0R are found to be relatively larger than those on ATZ-0.4R, despite the amount of strong acid sites on ATZ-0R being the same as that on ATZ-04R. According to Abelló et al. [40], this phenomenon could be attributed to the higher degree of Al extraction and redistribution on the mesopore surface of the zeolite desilicated with pure NaOH compared to that leached with the mixture of NaOH/TPAOH.

Noteworthy, even though the NH_3-TPD results show an increase in the acidity of treated samples, the acid sites strength (especially the strong acid sites) of these catalysts (ATZ-0R and ATZ-0.4R) is also slightly weakened as compared with that of the parent one, which is indicated by a shift of the ammonia desorption peaks center towards the lower temperatures after alkaline treatments (see Fig. 6 and Table 3). The decrease in the acid strength of protonic sites may be related to the extraction of some aluminum atoms from the zeolite framework in alkaline medium. Additionally, the presence of mesoporosity in these samples would help the removal of ammonia at lower temperatures, decreasing the strength of the acid sites as well. Such variation is consistent with the results reported in the literature for desilicated ZSM-5 materials [30,47]. However, appropriate concentration and strength of acid sites is crucial for improving the selectivity of propylene and the stability of the catalysts in the MTP reaction, which will be further discussed in the next section.

In brief, the characterization results indicate that the alkaline treatment of ZSM-5 creates materials with a micro-mesopore hierarchical structure without severely damaging the crystal structure and acidity of the zeolites, which could be expected to display a good catalytic performance in the transformation of methanol into light olefins.

3.2. Catalytic performance of the prepared catalysts in the MTP reaction

The influence of mesopore formation on the catalytic properties of desilicated ZSM-5 catalysts was tested in the methanol-to-propylene reaction. The catalytic performances of the parent and alkaline-treated ZSM-5 catalysts were evaluated in a continuous-flow fixed-bed reactor under the same operation conditions (T = 460 °C, P = 1 atm, and WHSV = 1 h^{-1}).

Table 4 displays full descriptions of products distributions in the conversion of methanol-to-propylene over the parent and alkaline-treated ZSM-5 catalysts in steady-state conditions when the catalysts yielded nearly full conversion and were presumably free from coke. The products obtained are classified into three groups. The first group contains lower paraffins, which include methane, ethane, propane, and butanes (C_1–C_4). The second group contains light olefins, which consist of ethylene, propylene, and total butylene ($C_2^= - C_4^=$). The last group contains heavier olefins, starting from pentene, as well as higher paraffins and aromatics such as benzene, toluene, and xylene (BTX), which are denoted by C_5^+. The catalytic performance of the parent ZSM-5 is ordinary. The parent ZSM-5 with Si/Al ratio of 175 delivers a propylene selectivity of 35.7% with a $C_2^= - C_4^=$ olefins selectivity of 69.2%, which is associated with the formation of a lot of C_1–C_4 alkanes (9.5%) and C_5^+ products (21.3%). This is possibly due to the high Si/Al ratio of the ZSM-5 zeolite employed in the present work, which presents a few strong acid sites. Earlier studies proved that the total acid sites of ZSM-5, especially the amount of strong acid sites, decreased with increasing the Si/Al ratio [10,14].

However, for this acid-catalyzed reaction (MTP), microporous ZSM-5 catalyst still tends to undergo rapid coking reactions, leading to the blockage of micropore channels and to catalyst deactivation [12]. Such contradiction would be well solved by the mesopore containing ZSM-5 catalyst. In this way, even with a lower Si/Al ratio, the mesoporous ZSM-5 catalyst is usable for a longer period of time than the conventional catalyst with a higher Si/Al ratio [14].

It can be clearly seen (Table 4) that compared with the parent ZSM-5, the alkali-treated catalysts (ATZ-xR samples) show noticeably higher selectivities to propylene and butylenes, while their selectivities toward ethylene, C_1–C_4

Table 4
Product distribution of MTP reaction over the parent and alkaline-treated ZSM-5 catalysts measured at steady state condition.

Catalyst	Conversion (%)	Selectivity (C-mol.%)					$C_2^= - C_4^=$	P/E
		C_{1-4}[a]	C_2H_4	C_3H_6	C_4H_8	C_5^+[b]		
Parent	99.9	9.5	13.2	35.7	20.3	21.3	69.2	2.70
ATZ-0R	99.8	8.1	11.8	39.8	23.4	16.9	75.0	3.37
ATZ-0.2R	99.7	7.1	10.6	43.9	25.6	12.8	80.0	4.14
ATZ-0.4R	99.8	5.7	9.5	47.2	27.9	9.7	84.6	4.97
ATZ-0.6R	99.7	6.7	10.3	44.4	26.2	12.4	80.8	4.31

[a] C_1–C_4 saturated hydrocarbons.
[b] C_5 and higher hydrocarbons.

alkanes, C_5^+ hydrocarbons are relatively lower. Detailed results show that, although propylene selectivity over ATZ-0R sample (39.8%) is better than that of the purely microporous parent sample (35.7%), it is still far from its optimal value. From the point of view of selectivity for propylene production, the catalytic performance of the hierarchical zeolites desilicated in the presence of TPAOH is superior in comparison to that of the material treated with pure NaOH (Table 4). However, various proportions between both bases (TPAOH and NaOH) also affect the initial catalytic activity of desilicated materials in the MTP process. Hence, with the increase in TPAOH/(TPAOH + NaOH) ratio of desilicating agent from 0.2 (ATZ-0.2R sample) to 0.4 (ATZ-0.4R sample), the propylene selectivity increases from 43.9% to 47.2%. But a further increase in the *R* ratio (ATZ-0.6R sample) is not beneficial, which also leads to decreases in propylene selectivity (44.4%). So, it is clear that the highest propylene production and total olefins selectivity (84.6%) are encountered with the ATZ-0.4R sample. Moreover, the ATZ-0.4R catalyst gives the best propylene-to-ethylene (P/E) ratio (4.97), which is a very important index parameter in the MTP process.

Moreover, catalytic stability was improved markedly upon alkaline treatment. Methanol conversion versus time on stream (TOS) over the parent and selected alkaline-treated ZSM-5 catalysts is shown in Fig. 7. Clearly, at the initial reaction period, due to the availability of the majority of acid sites for methanol, the parent and selected alkaline-treated ZSM-5 catalysts exhibited nearly full methanol conversion. However, when time on stream increases, all selected catalysts reduce their catalytic activity with different deactivation rates, which can be attributed to the different coverage of acid sites and the blockage of the pore mouth by carbon deposits based on the previous literature reports [31,32]. To obtain a quantitative estimate of the catalytic stability, the "catalytic lifetime" is defined as the time on stream at which the conversion of oxygenates (methanol and dimethyl ether) exceeded 90%, which is denoted by the dashed line in Fig. 7. From an industrial point of view, a conversion less than 90% is unacceptable for the MTP process and the catalyst should be regenerated or substituted [48].

The deactivation of parent ZSM-5 is rather fast and the methanol conversion falls below 90% after 43 h on stream. This is in very good agreement with the reported deactivation behavior of high-silica ZSM-5 in the literature [10]. The fast deactivation of the parent ZSM-5 can be explained by coke formation on the acid sites of the catalyst particles, gradually blocking the diffusion path of oxygenates (methanol and DME) to the active sites of the catalyst. In any fixed-bed catalyst operation, the portion of the catalyst bed that is in the downstream of the reaction front is deactivated by coking. As the reaction progresses with increased time, the deactivation front moves through the catalyst bed, until most of the catalyst bed is deactivated and the conversion drops rapidly after breakthrough of methanol (and DME) [8].

However, methanol conversion over the alkali-treated ZSM-5 catalysts exhibits enhanced catalytic lifetime (Fig. 7). The MTP lifetime values thus obtained for ATZ-0R and ATZ-0.4R are 63 h, and 80 h, respectively, which is higher than 43 h for the parent ZSM-5 catalyst. Especially for ATZ-0.4R, the catalytic lifetime is nearly twice longer than that of the parent catalyst. So, the lifetime of the

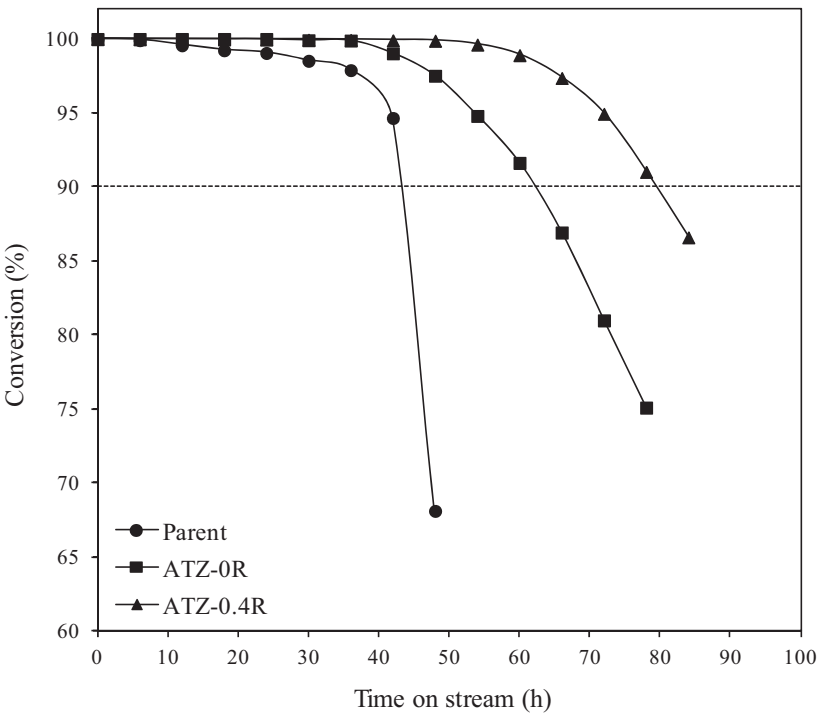

Fig. 7. Conversion of methanol as a function of time on stream over the parent and selected alkaline-treated ZSM-5 samples.

catalysts increases in the following order: parent (43 h) < ATZ-0R (63 h) < ATZ-0.4R (80 h). It is interesting to note that a similar improvement in the catalyst lifetime was previously reported by Milina et al. using a series of alkali-treated ZSM-5 zeolites during the methanol-to-hydrocarbon conversion [31,32].

The prominent difference in the catalytic performance of parent and alkali-treated ZSM-5 catalysts can be explained by the difference in the level of porosity and acidity as well as by the strength of the acid sites and accessibility of reactants to these active sites [13,30]. It has been reported that the significant changes in the acidity and the pore architecture of ZSM-5, resulting from the alkali treatment, could influence both the activity and the stability of the ZSM-5 catalyst in the MTH reaction [31–33]. Hence, it is necessary to understand the relationship between the catalyst's properties and catalytic performance before developing an effective catalyst.

Recent studies have proved that the acidity of the catalyst is one of the most important factors affecting the reactivity in the MTP reaction. It has been reported that the conversion of methanol to DME takes place mainly on the weak acid sites while the conversion of DME (and methanol) to light olefins occurs mainly on the strong acid sites [13,49]. Based on FT-IR and NMR studies, Campbell et al. [50] also indicated that the initial reactivity of methanol (the first C–C bond formation) is controlled by the concentration of Brønsted acid sites, and is not directly ruled by the concentration of extra-framework Al.

Based on the NH_3-TPD analysis results, both weak and strong acid site densities increase by alkaline treatments. Although, strong acid sites are the dominant active sites for MTP reaction, they also promote hydrogen transfer reaction of olefin to saturated hydrocarbons and aromatics, which are precursors of coke formation, which deactivates the catalysts [13,51]. So, the higher stability of alkali-treated ZSM-5 catalysts compared to the parent one cannot be explained by the increment of acidity. Nevertheless, as suggested by the NH_3-TPD results in Fig. 6 and Table 3, the distinct decrease in the strength of strong acid sites upon alkaline treatments, especially with the NaOH/TPAOH mixture (ATZ-0.4R sample), can alleviate the hydride transfer and cyclization reactions on strong acid sites that convert light olefins to paraffins, aromatics, naphthenes, and higher olefins. Consequently, the coke precursor condensation steps are also attenuated, and therefore deactivation is minimized [13,34,52]. These results indicate that weakening the acid strength of the ZSM-5 zeolites upon alkaline treatments can effectively improve the MTP catalytic lifetime.

However, the marked discrepancy between the lifetimes of parent and desilicated catalysts in the mass transfer-limited reaction of methanol to hydrocarbons cannot be rationalized only on the basis of the acidic properties. Beside the acidic properties of zeolite catalysts, structural properties such as pore size distribution and channel length also play a key role on the stability of the alkali-treated ZSM-5 catalysts [13,53]. Since the majority of the active sites of the parent ZSM-5 catalysts are located in its micropore channels, it thus has a particular shape selectivity. Hence, only the reaction-produced molecules whose size is smaller than that of ZSM-5 channels can diffuse out as reaction products. The larger spices would be more likely to become trapped and thereby form a coke precursor. So, the solely microporous ZSM-5 catalyst is progressively deactivated as the micropores are filled with coke deposits, or their entrances become blocked [54]. In contrast, in the case of hierarchical structured zeolites (alkali-treated) with intra- and/or intercrystalline mesoporosity, coke is formed mainly on the external surface and/or mesopores. Considerably high mesoporosity and shorter diffusion path length in the alkali-treated ZSM-5 catalysts facilitate the transfer of the coke precursor towards the outside of the micropores, attenuating coke deposition in the micropore channels even at a high coking level. Consequently, the slight coke deposition and the lesser susceptibility to form more coke deposits can contribute to the slowing down of the deactivation of alkali-treated catalysts that ensures the operation of long-term methanol conversion into light olefins [31–33,55].

The outstanding diffusivity of the alkalie-treated ZSM-5 catalysts has also a great effect on their product distribution in MTP reaction, which facilitates the removal of the intermediate products, particularly propylene and butylene with larger molecular sizes, from the reactive centers of the catalysts. As a result, the reaction equilibrium shifts to the formation of propylene and butylene, and also the probability that these olefins further form higher olefins, paraffins, aromatics and naphthenes via various secondary reactions on the acid sites of the catalysts is reduced [31,33,55]. Thus, the selectivities to propylene and butylene as well as the P/E ratio over alkali-treated ZSM-5 catalysts are enhanced as compared with the parent microporous ZSM-5 catalyst (see Table 4), while selectivities to other products, including C_1–C_4 alkanes, ethylene and C_5^+ hydrocarbons (including aromatics), are decreased, which corresponds to the hydrocarbon pool mechanism. According to this mechanism, there are two possible hydrocarbon pool cycles on ZSM-5 catalyst, C_3^+ alkenes methylation and cracking cycle (olefin-based cycle) and (poly)methylbenzene methylation and dealkylation cycle (aromatic-based cycle) [56]. Propylene and higher alkenes are mainly formed through the olefin-based cycle, whereas ethylene is predominantly formed from the aromatic-based cycle. Due to this inference, with the improvement of diffusivity, the residence time of the (poly)methylbenzene intermediates in the microporous reaction zone is shorter in the desilicated samples, leading to less secondary dealkylation reactions, then the formation of ethylene is diminished and the olefin-based cycle plays a major role in the MTP reaction [57,58]. Therefore, noticeably higher propylene selectivity and higher P/E ratio were achieved with the alkali-treated ZSM-5 catalysts.

It should be noted that the increase in the number of strong acid sites after alkaline treatment may be favorable to a higher propylene selectivity and P/E ratio in MTP reaction over hierarchical mesoporours ZSM-5 catalysts. Increased numbers of strong acid sites allow one to increase the opportunities for the MTO reaction (C–C bond formation) and the mesopore structure accelerates the removing of primary olefins from the catalyst's pores. So,

the aromatic-based cycle is suppressed while the olefin-based cycle is dominated, which enhances propylene selectivity and P/E ratio [13,58].

Furthermore, the NH_3-TPD results (Table 3) also present higher amounts of weak acid sites for alkali-treated ZSM-5 catalysts (ATZ-0R and ATZ-0.4R samples) compared to the parent one, which may also promote propylene production (Table 4) and improve MTP catalytic stability (Fig. 7). The weak acidity, in addition to the fact that the catalyst participates in the conversion of methanol to dimethyl ether, can also catalyze the alkylation and methylation reactions, which highly influences propylene selectivity according to the dual-cycle concept [49,57,59]. Moreover, weak acid sites efficiently hinder various side-reactions producing saturated hydrocarbons and aromatics (C_5^+). Consequently, alkali-treated catalysts with higher weak acid sites exhibit better anti-coking capability than that of parent ZSM-5 catalyst for long-term stability in the MTP reaction [13,49].

Finally, our main conclusion is that the ZSM-5 zeolite treated with a mixture of NaOH/TPAOH represents the best catalytic performance, including the highest propylene selectivity and P/E ratio as well as the longest catalyst lifetime, among all the studied catalysts. From a catalytic point of view, not only the accessibility of the active centers of the catalyst is important, but the number and strength of the acid sites are also essential factors [30]. Hence, the best catalytic performance for the MTP reaction over the NaOH/TPAOH-treated ZSM-5 catalyst (ATZ-0.4R) could be attributed to well-developed mesopores (only intracrystalline mesopores) with the highest hierarchy factor (0.195), which will shorten the diffusion path and improve the accessibility of reactants to reactive sites as well as reduce the strength of acid sites without altering the intrinsic acidity of high-silica ZSM-5 [60].

4. Conclusions

In this work, the physicochemical properties and MTP catalytic performance of high-silica ZSM-5 zeolites (Si/Al = 175) modified with pure NaOH or a mixture of NaOH and TPAOH have been investigated, and the results have been compared to those of the parent ZSM-5. The characterization results reveal that the alkaline treatment of ZSM-5 zeolite leads to the formation of a hierarchical porosity as well as to a reduction in the strength of the acid sites without severely damaging the crystal structure and intrinsic acidity of the zeolite. Additionally, it is demonstrated that the presence of TPA^+ cations in the alkaline medium results in the formation of a narrower and uniform mesopore size distribution size distribution compared to the one obtained by treatment in pure NaOH. Nevertheless, the high concentration of TPA^+ is not beneficial to the development of further mesoporosity. Hence, the ZSM-5 zeolite treated with TPAOH/(NaOH + TPAOH) = 0.4 represents the best catalytic performance, including the highest propylene selectivity (47.2) and P/E ratio (4.97) as well as longest catalyst lifetime (80 h) in the catalytic conversion of methanol to propylene among all catalyst samples. The lower strength of its acid sites as well as the better accessibility of the reactants to its reactive centers due to its well-developed mesopores, leading to the propagation of the olefin-based cycle over the aromatic-based cycle in methanol-to-hydrocarbon catalysis, could be the reasons to explain the better catalytic performance of ATZ-0.4R catalyst.

Acknowledgments

We would like to acknowledge the Iranian Nano Technology Initiative Council for financial support of this work.

References

[1] M. Firoozi, M. Baghalha, M. Asadi, Catal. Commun. 10 (2009) 1582.
[2] C. Mei, P. Wen, Z. Liu, H. Liu, Y. Wang, W. Yang, Z. Xie, W. Hua, Z. Gao, J. Catal. 258 (2008) 243.
[3] P. Losch, M. Boltz, B. Louis, S. Chavan, U. Olsbye, C. R. Chimie 18 (2015) 330–335.
[4] Z.S. Barros, F.M.Z. Zotin, C.A. Henriques, Stud. Surf. Sci. Catal. 167 (2007) 255.
[5] F. Yaripour, Z. Shariatinia, S. Sahebdelfar, A. Irandoukht, J. Nat. Gas Sci. Eng. 22 (2015) 260.
[6] N. Hadi, A. Niaei, S.R. Nabavi, A. Farzi, M.N. Shirazia, Chem. Biochem. Eng. Q 28 (2014) 53.
[7] T. Mokrani, M. Scurrell, Catal. Rev. 51 (2009) 1.
[8] U.V. Mentzel, K.T. Højholt, M.S. Holm, R. Fehrmann, P. Beato, Appl. Catal. A: Gen. 417–418 (2012) 290.
[9] C.D. Chang, C.T.W. Chu, R.F. Socha, J. Catal. 86 (1984) 289.
[10] J. Liu, C. Zhang, Z. Shen, W. Hua, Y. Tang, W. Shen, Y. Yue, H. Xu, Catal. Commun. 10 (2009) 1506.
[11] S. Hu, J. Shan, Q. Zhang, Y. Wang, Y.S. Liu, Y.J. Gong, Z.J. Wu, T. Dou, Appl. Catal. A: Gen. 445 (2012) 215.
[12] Z. Hu, H. Zhang, L. Wang, H. Zhang, Y. Zhang, H. Xu, W. Shen, Y. Tang, Catal. Sci. Technol. 4 (2014) 2891.
[13] F. Yaripour, Z. Shariatinia, S. Sahebdelfar, A. Irandoukht, Micropor. Mesopor. Mater. 203 (2015) 41.
[14] C. Sun, J. Du, J. Liu, Y. Yang, N. Ren, W. Shen, H. Xu, Y. Tang, Chem. Commun. 46 (2010) 2671.
[15] K. Moller, T. Bein, Chem. Soc. Rev. 42 (2013) 3689.
[16] D.P. Serrano, J.M. Escola, P. Pizarro, Chem. Soc. Rev. 42 (2013) 4004.
[17] J.C. Groen, J.C. Jansen, J.A. Moulijn, J. Pérez-Ramírez, J. Phys. Chem. B 108 (2004) 13062.
[18] J.C. Groen, J.A. Moulijn, J. Pérez-Ramírez, J. Mater. Chem. 16 (2006) 2121.
[19] D. Verboekend, J. Pérez-Ramírez, Chem. – Eur. J. 17 (2011) 1137.
[20] D. Verboekend, S. Mitchell, M. Milina, J.C. Groen, J. Pérez-Ramírez, J. Phys. Chem. C 115 (29) (2011) 14193.
[21] V. Rac, V. Rakić, Z. Miladinović, D. Stošić, A. Auroux, Thermochim. Acta 567 (2013) 73.
[22] D. Verboekend, J. Pérez-Ramírez, Catal. Sci. Technol. 1 (6) (2011) 879.
[23] M.-L. Goub, R. Wanga, Q. Qiaoa, X. Yang, Micropor. Mesopor. Mater. 206 (2015) 170.
[24] K. Sadowska, A. Wach, Z. Olejniczak, P. Kuśtrowski, J. Datka, Micropor. Mesopor. Mater. 167 (2013) 82.
[25] K. Góra-Marek, K. Tarach, J. Tekla, Z. Olejniczak, P. Kuśtrowski, L. Liu, F. Rey, J. Phys. Chem. C 118 (2014) 28043.
[26] D. Tzoulaki, A. Jentys, J. Pérez-Ramírez, K. Egeblad, J.A. Lercher, Catal. Today 198 (2012) 3.
[27] K. MLekodaj, K. Sadowska, J. Datka, K. Góra-Marek, W. Makowski, Micropor. Mesopor. Mater. 183 (2014) 54.
[28] K. Sadowska, K. Góra-Marek, J. Datka, J. Phys. Chem. C 117 (2013) 9237.
[29] J. Pérez-Ramírez, D. Verboekend, A. Bonilla, S. Abelló, Adv. Funct. Mater. 9 (2009) 3972.
[30] K. Sadowska, K. Góra-Marek, M. Drozdek, P. Kuśtrowski, J. Datka, J. Martinez-Triguero, F. Rey, Micropor. Mesopor. Mater. 168 (2013) 195.
[31] M. Milina, S. Mitchell, P. Crivelli, D. Cooke, J. Pérez-Ramírez, Nat. Commun. 5 (2014) 3922, http://dx.doi.org/10.1038/ncomms4922.
[32] M. Milina, S. Mitchell, D. Cooke, P. Crivelli, J. Pérez-Ramírez, Angew, Chem. Int. Ed. (2014), http://dx.doi.org/10.1002/anie.201410016.
[33] M. Bjørgen, F. Joensen, M.S. Holm, U. Olsbye, K.P. Lillerud, S. Svelle, Appl. Catal. A 345 (2008) 43.
[34] Y.P. He, M. Liu, C.Y. Dai, S.T. Xu, Y.X. Wei, Z.M. Liu, X.W. Guo, Chin. J. Catal. 34 (2013) 1148.

[35] S. Li, Y.P. Li, C.Y. Di, P.F. Zhang, R.L. Pan, T. Dou, J. Fuel Chem. Technol. 40 (2012) 583.
[36] J. Ahmadpour, M. Taghizadeh, J. Nat. Gas Sci. Eng. 23 (2015) 184.
[37] ASTM Standard Test Method D5758-01 2011.
[38] D. Verboekend, G. Vile, J. Pérez-Ramírez, Cryst. Growth Des. 12 (2012) 3123.
[39] J.C. Groen, L.A.A. Peffer, J.A. Moulijn, J. Pérez-Ramírez, Chem. – Eur. J. 11 (2005) 4983.
[40] S. Abelló, A. Bonilla, J. Pérez-Ramírez, Appl. Catal. A 364 (2009) 191.
[41] G. Coudurier, J.C. Vedrine, Pure Appl. Chem. 58 (1986) 1389.
[42] G.V.A. Martins, G. Berlier, C. Bisio, S. Coluccia, H.O. Pastore, L. Marchese, J. Phys. Chem. C 112 (2008) 7193.
[43] A. Martin, H. Berndt, React. Kinet. Mech. Catal. 52 (1994) 405.
[44] U. Olsbye, S. Svelle, M. Bjorgen, P. Beato, T.V.W. Janssens, F. Joensen, S. Bordiga, K.P. Lillerud, Angew. Chem. Int. Ed. 51 (2012) 5810.
[45] V. Van Speybroeck, K. De Wispelaere, J. Van der Mynsbrugge, M. Vandichel, K. Hemelsoet, M. Waroquier, Chem. Soc. Rev. 43 (2014) 7326.
[46] Y.Q. Song, Y.L. Feng, F. Liu, C.L. Kang, X.L. Zhou, L.Y. Xu, G.X. Yu, J. Mol. Catal. A: Chem. 310 (2009) 130.
[47] A.N.C. Van Laak, L. Zhang, A.N. Parvulescu, P.C.A. Bruijnincx, B.M. Weckhuysen, K.P. De Jong, P.E. De Jongh, Catal. Today 168 (2011) 48.
[48] M. Rostamizadeh, A. Taeb, J. Ind. Eng. Chem. (2015), http://dx.doi.org/10.1016/j.jiec.2015.01.004.
[49] Y. Yang, C. Sun, J. Du, Y. Yue, W. Hua, C. Zhang, W. Shen, H. Xu, Catal. Commun. 24 (2012) 44.
[50] S.M. Campbell, X.-Z. Jiang, R.F. Howe, Micropor. Mesopor. Mater. 29 (1999) 91.
[51] T. Mole, J.A. Whiteside, J. Catal. 75 (1982) 284.
[52] S.H. Zhang, Z.X. Gao, S.Y. Liu, Y.Z. Han, Y.S. Zhao, Chem. Eng. Technol. 34 (2011) 1700.
[53] M. Dyballa, E. Klemm, J. Weitkamp, M. Hunger, Chem. Ing. Tech. 85 (2013) 1719.
[54] Z. Wan, W. Wu, W. Chen, H. Yang, D. Zhang, Ind. Eng. Chem. Res. 53 (2014) 19471.
[55] S. Mitchell, N.-L. Michels, K. Kunze, J. Pérez-Ramírez, Nat. Chem. 4 (2012) 825.
[56] S. Svelle, F. Joensen, J. Nerlov, U. Olsbye, K.P. Lillerud, S. Kolboe, M. Bjørgen, J. Am. Chem. Soc. 128 (2006) 14770.
[57] S. Zhang, Y. Gong, L. Zhang, Y. Liu, T. Dou, J. Xu, F. Deng, Fuel Process. Technol. 129 (2015) 130.
[58] M. Wen, X. Wang, L. Han, J. Ding, Y. Sun, Y. Liu, Y. Lu, Micropor. Mesopor. Mater. 206 (2015) 8.
[59] Q.J. Zhu, J.N. Kondo, T. Setoyama, M. Yamaguchi, K. Domen, T. Tatsumi, Catal. Commun. 5164 (2008).
[60] K. Tarach, K. Góra-Marek, J. Tekla, K. Brylewska, J. Datka, K. MLekodaj, W. Makowski, M.C. Igualada López, J. Martínez Triguero, F. Rey, J. Catal. 312 (2014) 46.